

Monolithic InGaAs JFET Active Pixel Tunable Image Sensor (MATIS)

Q. Kim, T. J. Cunningham, and E. R. Fossum[†]

Center for Space Microelectronics Technology
Jet Propulsion Laboratory
California Institute of Technology
Pasadena, California 91109

[†] Photobit, La Crescenta, CA 91214

ABSTRACT

A new Monolithic InGaAs Active Pixel Multispectral Image Sensor is described. This Infrared sensor will utilize high quality InGaAs grown by Molecular Beam Epitaxy on InP substrate for the fabrication of a high speed Junction Field Effect Transistor array. In $_{1-x}$ Ga $_x$ As is a III-V alloy whose cutoff wavelength can be tuned from 0.8 μ m (GaAs) to 3.5 μ m (InAs). Due to the spectral windows of 3-5 μ m and 8-12 μ m in atmosphere, this material has not received much attention to date for infrared focal plane arrays even though the responsivities for the 0.8-1.0 μ m, and 2.0-2.5 μ m windows for the water and carbon dioxide molecules in air are excellent. Steady advancements of InGaAs material growth and devices have been made, primarily driven by the optoelectronics industry and the high speed electronics community. Most of this knowledge exists in the public domain and is readily accessible. Detectors at 1.7 μ m cutoff can be ideally implemented as lattice matched In $_{0.53}$ Ga $_{0.47}$ As/InP PIN devices. PIN detectors require high material quality to reduce dark current and decrease bit errors. Additionally, the high intrinsic mobility of In $_{0.53}$ Ga $_{0.47}$ As enables very high speed transistors for monolithic microwave integrated circuit applications. The new Active Pixel Sensor technology, a likely successor to charge coupled device, has developed for low noise, high signal transfer efficiency imaging circuits at JPL. In this exploratory development efforts, a preliminary result of a monolithic multispectral (visible/near infrared/short-wavelength infrared) imaging sensor will be discussed for application in transportable shipboard surveillance, night vision and emission spectroscopy.

Keywords: Hyper spectral responses, Monolithic, Near room temperature, Active pixel sensor

INTRODUCTION

Junction field effect transistors (JFETs) in III-V semiconductor applications have received considerable attention for application in high speed digital very large scale integrated (VLSI) systems due to the recent advancement of its material quality and fabrication technology.^{1,5} The JFET technology can reduce the gate leakage current which affects many aspects of the device performance of the noise margin, power dissipation, and the speed, caused by the low gate turn on voltage of the Schottky barrier in conventional direct-coupled field effect transistor (JFET) logic.^{6,7}

Furthermore, the advancement of InGaAs heterostructure field effect transistors on InP and continued advancement in micro lithography feature size reduction for the production of semiconductor circuits, such as dynamic random access memories (DRAMs) and microprocessors, enable the consideration of a new image sensor technology, called the Active Pixel Sensor (APS). In the new APS, one or more active transistors are integrated into the pixel of an imaging detector, and buffer the photosignal as well as drive the read out lines. In any instant, only one row is active, so that power dissipation in the APS is less than that of a charge coupled device (CCD). The physical fill-factor of the APS can be approximately 30% or higher, and the use of on-chip microlenses or binary optics can increase the effective fill-

factor to 70%. Sensitivity, readout noise, and dynamic range are similar to the $(1/f)$. Thus the APS preserves the high performance of the $(1/f)$ but eliminates the need for the burden of almost perfect charge transfer. The APS technology is just emerging in the most advanced imager laboratories in Japan for application to high-definition television (111) $1/V$ and electronic still cameras.⁸

For earth and planetary remote sensing applications, there are a broad range of scientifically important measurements to be made in the visible ($0.4 - 0.7 \mu\text{m}$; Vis), near infrared ($0.7 - 1.0 \mu\text{m}$; NIR), and short-wavelength infrared ($1.0 - 2.5 \mu\text{m}$, SWIR). The principle reason for the importance of the wavelength regions is that they span the region of peak solar illumination. In this region, the primary phenomenology of interest is the reflectance signature of the intended target, manifested as either brightness variations, spectral reflectance variations, or both. The most commonly known subset of this group of applications is the simple electronic imaging system, of which some variant has been flown on virtually every scientific space mission. Imaging systems perform a wide variety of important measurements ranging from assessing the overall brightness, composition, and texture of the surface, to deducing atmospheric density and composition. Addition of multiple spectral filters has increased the information returned by these systems. The sophistication of traditional imaging systems has evolved along a variety of routes: increased spatial resolution (of particular interest to the intelligence community); broader wavelength coverage, particularly in the infrared; and incorporation of traditional laboratory spectroscopy techniques in which materials are identified through their unique spectral signatures. This latter trend has led to the emergence of the imaging spectrometry concept described earlier. The SWIR provides a particularly fertile region for new and important scientific measurements: there is substantial natural illumination available from the sun; there are a broad variety of materials with unique spectral signatures in this region; and there are a variety of mature detector technologies available. Many different instruments are in operation or under construction for both earth and planetary remote sensing applications.^{9,10}

The needs of InGaAs infrared (IR) array can make a significant impact on the implementation and miniaturization of shipboard surveillance, night vision, and emission spectroscopy instruments in space. A lower dark current linear array in both visible and, especially IR spectral regime, comparing with HgCdTe, would likely be the great interest in the design of scientific miniature spectrometer, machine vision and smart sensor application. While the development of a high performance $2.5 \mu\text{m}$ InGaAs array is dependent on control of lattice-mismatch during material growth, other wavelength such as $1.7 \mu\text{m}$ InGaAs is considered an off-the-shelf technology. In principle, III-V compound semiconductor material growth is easier to control than II-VI ternary material growth. Many commercial companies have successfully developed epitaxial growing techniques of high quality III-V semiconductor materials, while continued support of $2.5 \mu\text{m}$ InGaAs material development will be required to realize the potential for the future scientific application. Monolithic APS is an approach to overcome both the hybridization to a silicon multiplexer noise to enable focal-plane application and the back-side illumination of the visible response in two dimensional silicon array hybridization scheme.

This paper describes InGaAs APS detector technology. Section 2 reviews the potential advantages of the InGaAs imaging system as a potential hyper spectral imaging system. Section 3 describes the key concepts of the design and operation of CMOS active pixel image sensors. Section 4 describes the projected goals, plans and challenges as well as some preliminary characterization results of the fundamental InGaAs APS device structures.

2. MONOLITHIC InGaAs JFET

2.1 InGaAs Growth for Multi-spectral Response

The ternary $\text{In}_x\text{Ga}_{1-x}\text{As}$ can be grown epitaxially on a III-V binary substrate. As the indium mole fraction, x , varies from $x = 0$ (pure GaAs) to $x = 1$ (pure InAs) the bandgap varies continuously from $E_g = 1.424 \text{ eV}$ to $E_g = 0.360 \text{ eV}$, respectively. The longest wavelength to which the device is sensitive, called the cut-off wavelength λ_{co} correspondingly varies from $\lambda_{co} = 0.8 \mu\text{m}$ to $\lambda_{co} = 3.5 \mu\text{m}$, respectively. At any given temperature, the device dark current increases as E_g decreases because of the smaller barrier to thermal generation of electron-hole pairs. This provides the designer with a trade-off between λ_{co} and the dark current, which the designer can optimize for a particular application by selecting the proper indium mole fraction.

InGaAs with an indium mole fraction of 0.53 is lattice-matched to InP, and so can be grown sIrdir-free on an InP substrate^{11,12}. This fixed mole fraction limits the designer to a specific cut-off wavelength, which happens to be $\lambda_{co} = 1.7 \mu\text{m}$ for $\text{In}_{0.53}\text{Ga}_{0.47}\text{As}$. Detectors with an $\text{In}_{0.53}\text{Ga}_{0.47}\text{As}$ active region grown on InP substrates have been made with dark current densities (at -5V) of less than $1 \mu\text{A}/\text{cm}^2$, quantum efficiencies greater than 70%, $D^*\text{ values greater than } 10^{12} \text{ CM}^2/\text{Hz}^{1/2}$, and subnanosecond rise-times at room temperatures. The dark current can be reduced by more than 200 times just with thermoelectric cooling.

In order to fabricate detectors with $\lambda_{co} > 1.7 \mu\text{m}$, the indium mole fraction can be increased beyond 0.53, but this requires some scheme to relax the strain. The superlattice consists of layers on the order of $1 \mu\text{m}$ thickness. The lattice constant of the layer that is closest to the substrate is equal to or only slightly different from the substrate (see Figure 1). Each layer grown after that has a lattice constant closer to the InGaAs active region. Dislocations that relax the strain are generated in the thick buffer layer, but are trapped by the abrupt heterojunctions between superlattice layers, so that the dislocations do not continue into the active region, leaving it with a low defect density. Detectors with strain-relaxed InGaAs active layers with indium mole fractions up to 0.87 have been grown using the superlattice buffer technique on an InP substrate^{11,13}. This technique has also been used to grow strain-relaxed InGaAs on a GaAs substrate^{14,17}. At this time, the largest indium mole fraction that has been reported for strain-relaxed InGaAs on a GaAs substrate is 0.40, which is less than the 0.53 mole fraction of sIrdir-free InGaAs on InP.

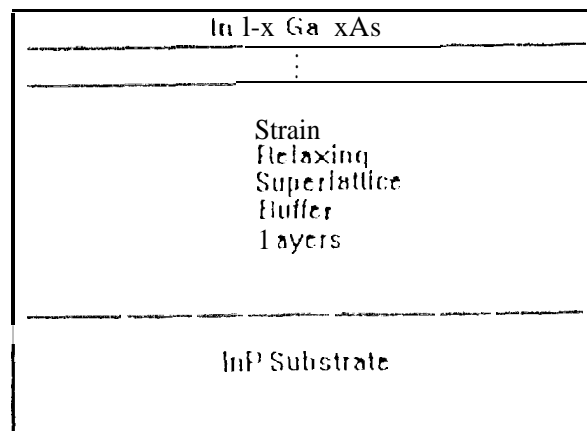


Figure 1. Stress Relaxed InGaAs Sensor Structure.

Hydride vapor phase epitaxy (VPE) has been used to grow low dark current InGaAs photodiodes on InP substrates with indium mole fractions ranging from 0.53 to 0.82. Molecular beam epitaxy (MBE) has been used successfully to grow strain-relaxed InGaAs on GaAs substrates. Kavanagh, *et al.*, grew $\text{In}_{0.3}\text{Ga}_{0.7}\text{As}$ on a GaAs substrate with a dislocation density of less than $2 \times 10^5/\text{cm}^2$ and used such material to form an $\text{In}_{0.3}\text{Ga}_{0.7}\text{As}/\text{In}_{0.29}\text{Al}_{0.71}\text{As}$ heterostructure¹³⁻¹⁴. Such material was then successfully used to make a HET¹⁵. Rogers, *et al.*, have also fabricated strain-relaxed $\text{In}_{0.4}\text{Ga}_{0.6}\text{As}$ metal-semiconductor-metal (MSM) detectors with a cut-off wavelength of $1.3 \mu\text{m}$ on GaAs substrates¹⁶. These MSM detectors had a bandwidth of up to 3 GHz. Ban, *et al.*, compared the results of lattice-matched InGaAs p-i-n detectors on InP substrates grown by hydride VPE and metallorganic chemical deposition (MOCVD). They found that both methods were capable of fabricating commercial quality devices with over 90% wafer yield¹⁸.

Fabrication technology has also been steadily improved. Recently, low contact transfer resistance to a GaInAs/InP composite channel was reported using nonalloyed regrown N^+ contact regions by MOCVD. Regrown channel contacts were used to achieve low contact resistance (0.35 $\Omega\text{-mm}$) to (50 A) InGaAs/ (150 A) InP composite channel high electron mobility transistors. High transconductance (600 mS/mm), high full channel current (650 mA/mm), and high peak cut-off frequencies ($f_{\text{ft}} = 70 \text{ GHz}$, $f_{\text{max}} = 170 \text{ GHz}$) were also observed.¹⁹

2.2 Near Room Temperature Operation

In infrared instruments covering the SWIR region, cooling is necessary only to reduce the dark current of the detector. The background photon signal from the warm instrument is almost negligible, except perhaps at the longest wavelengths. No cooling of the optical system is needed. In such a low background environment, the focal plane sensitivity is ultimately determined by the R_0A product of the photodiode. The most commonly used detector technologies in this region are indium antimonide (InSb) and mercury cadmium telluride (MCT) photovoltaic detectors. InSb requires cooling down to less than 80K, (due to its small bandgap ($\lambda_{co} = 53 \mu m$); care must be taken to ensure that background at wavelengths longer than $2.5 \mu m$ is filtered out. For MCT, the alloy concentration can be fixed to provide a bandgap equal to the longest wavelength to be observed (Hg_{0.5}Cd_{0.5}Te at $2.5 \mu m$). The larger bandgap allows higher temperature operation. There are continued efforts to increase the operating temperature of SWIR MCT detectors.

Infrared detectors based on InGaAs alloys offer a solution to the contradictory demands of high sensitivity and high operating temperature. Along with higher temperature operation come further possible benefits: visible response and monolithic arrays. InGaAs material has not received much attention for scientific focal planes, primarily since it cannot respond in the $3.5 \mu m$ to $12 \mu m$ atmospheric windows as MCT. However, it is a much easier material system in many respects than MCT, which translates into potentially higher figures of merit. InGaAs detectors that have been fabricated and tested already show large advantages over corresponding MCT detectors. A typical InGaAs photodetector structure is shown in figure 1.

2.3 Front Illumination

Integration of the readout with the photodetector has worked very well in silicon, but attempts at monolithic MCT arrays have met with limited success at best. Research into circuit elements based on InGaAs, however, shows that high quality components are possible.¹⁹ Junction field effect transistors (JFETs) and charge coupled devices (CCDs) with high performance have already been demonstrated in InGaAs. With these elements, an infrared focal plane consisting of photodiodes and an integrated readout is feasible.

A focal plane capable of operating in both the visible and the SWIR eliminates these constraints, resulting in a much more simple and compact instrument. InGaAs detectors have been fabricated in frontside illuminated configurations that offer excellent infrared response and good visible response. Good quantum efficiency down to $0.7 \mu m$ was demonstrated on a spectrum of an InGaAs detector ($\lambda_{co} = 1.7 \mu m$), limited only by the InP cap layer over the pixel. This cap layer is deposited epitaxially and can easily be grown thinner, or eliminated, to further enhance the visible response. Further research into different passivation layers for the InGaAs surface will lead to anti-reflection coatings in order to increase the light into the active region of the diode. The result of these advances should be a focal plane responsive from below $2.5 \mu m$ with high quantum efficiency: ideal for many earth remote sensing applications.

2.4 Miniature Imaging System

Miniaturization of instruments operating in the SWIR is important as an enabling technology for a wide variety of applications. For planetary exploration, for example, mission concepts are under development for a fast flyby of Pluto using a small spacecraft. Additionally, the characterization of the Mars environment through the use of an array of small sensors dropped to the surface is being developed. For Earth remote sensing, miniature instruments will be important for field measurements, operation on light aircraft, and a variety of other mobile surveillance applications.²⁰

3. CMOS ACTIVE PIXEL IMAGE SENSORS

In many imaging systems, integration of the image sensor with circuitry for both driving the image sensor and performing on-chip signal processing is becoming increasingly important. A high degree of electronics integration on the

focal-plane can enable miniaturization of instrument systems and simplify system interfaces. In addition to good imaging performance with low noise, no lag, no smear and good blooming control, it is desirable to have random access, simple clocks and fast readout rates. The development of a complementary metal-oxide semiconductor (CMOS)-compatible image sensor technology is an important step for highly integrated miniature imaging systems since CMOS is well-suited for implementing on-chip signal processing circuits. CMOS is also a widely accessible and well-understood technology.

CCDs are currently the dominant technology for image sensors. CCD arrays with high fill-factor, small pixel sizes and large formats have been achieved and some signal processing operations have been demonstrated with charge-domain circuits.²¹⁻²³ However, CCDs cannot be easily integrated with CMOS circuits due to additional fabrication complexity and increased cost. Also, CCDs are high capacitance devices so that on-chip CMOS drive electronics would dissipate prohibitively high power levels for large area arrays (2-3 W). Furthermore, CCDs need many different voltage levels to ensure high charge transfer efficiency. The readout rate is limited due to the inherent sequential readout of the $\sim 10^6$ elements and the need to achieve nearly perfect charge transfer efficiency to maintain signal fidelity. CCDs also suffer from smear and susceptibility to radiation damage.

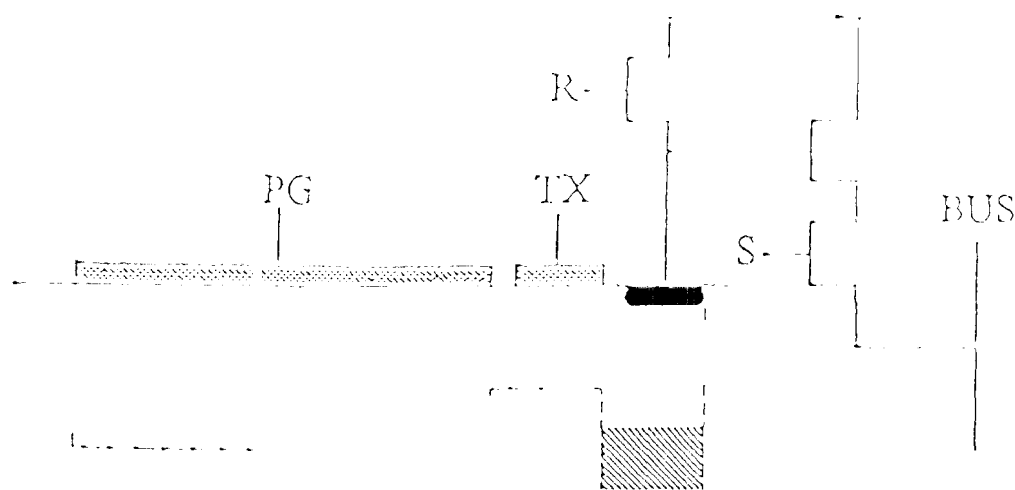


Fig. 2 JPI Active Pixel Sensor (APS).

An active pixel image sensor is defined as an image sensor technology that has one or more active transistors within the pixel unit cell.⁸ (see Figure 2) This is in contrast to a passive pixel approach that uses a simple switch to connect the pixel signal charge to the column bus capacitance.²⁴ Active pixel sensors demonstrated lower noise readout, improved scalability to large array formats and higher speed readout compared to passive pixel sensors. Previously demonstrated active pixel sensor technologies include the amplified metal-oxide semiconductor imager (AMI),²⁵ charge modulation device (CMD),²⁶ bulk charge modulated device (BCMD),²⁷ base stored image sensor (BASIS)²⁸ and the static induction transistor (SIT).²⁹ Although AMIs are both CMOS-compatible and liable to integration with on-chip circuitry, noise levels and lag can be a problem due to the uncorrelated reset operation.³⁰ CMDs, BCMDs and BASIS are also amenable to integration with on-chip circuitry, but can be made CMOS compatible only with additional fabrication steps. SITs are difficult to integrate with on-chip circuitry and are not CMOS compatible.

The CMOS active pixel sensors described in previous report³¹ are inherently CMOS-compatible. Each pixel unit cell contains an imaging element and three transistors for readout, selection and reset. The imager is read out a row at a time using a column parallel readout architecture. The major innovation reported in previous paper is the use of intra-pixel charge transfer to allow correlated-double-sampling (CCDS) and on-chip fixed pattern noise (FPN) suppression circuitry located in each column. Those innovations will allow, for the first time, a CMOS image sensor to achieve low noise performance comparable to a CCD. In all the designs random access is possible, allowing selective readout of windows of interest. The image sensors are operated with transistor-transistor logic clocks and at most two other direct current voltages. These image sensors achieved lateral blooming control through proper biasing of the reset transistor. No lag or smear was

evident. The reset and signal levels are read out differentially, allowing CDS to suppress kTC noise, 1/f noise and fixed pattern noise from the pixel. Low noise and high dynamic range were achieved. The use of a radiation hard CMOS process to implement the sensor is also a possibility. The CMOS active pixel image sensors reported earlier had performance suitable for many applications including robotics and machine vision, guidance and navigation, automotive applications, and consumer electronics such as video phones, computer inputs and home surveillance devices. Future development will lead to both transportable shipboard surveillance and scientific sensors suitable for highly integrated imaging systems for NASA deep space, planetary spacecraft and mobile field camera.

A schematic of the basic pixel design and readout circuit used in the CMOS APS arrays is shown in Fig. 3. The pixel unit cell is shown within the dotted outline. The imaging structure consists of a photogate (PG) with a floating diffusion output (FD) separated by a transfer gate (TX). In essence, a small surface-channel CCD has been fabricated within each pixel. The pixel unit cell also contains a reset transistor (MR), the input transistor of the in-pixel source-follower (MIN) and a row selection transistor (MX).

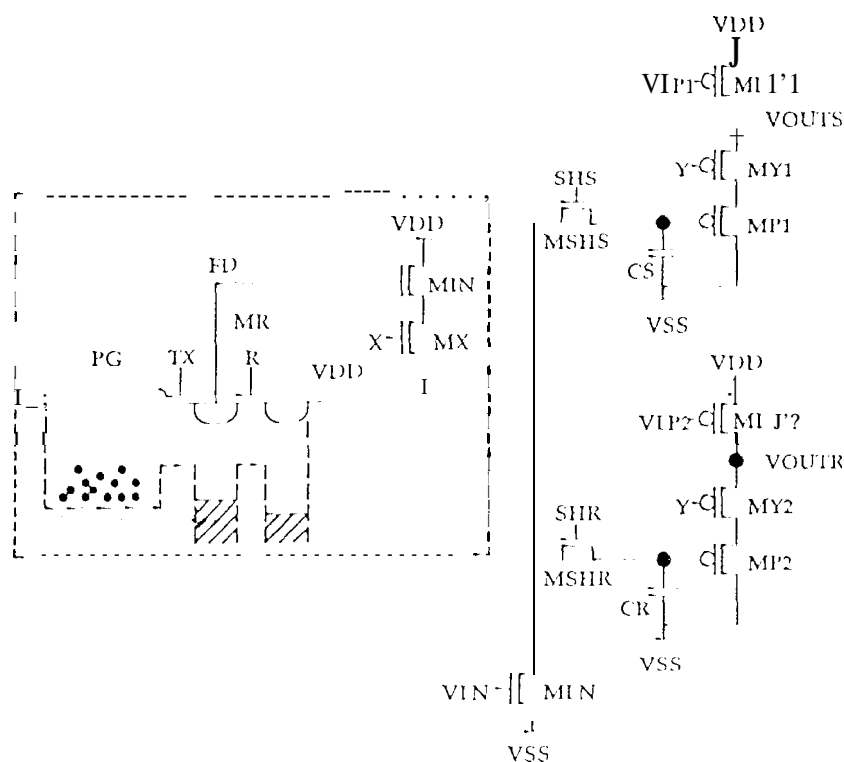


Figure 3. Schematic of Readout Circuit of CMOS APS

The readout circuit, which is common to an entire column of pixels, includes the load transistor of the first source-follower (MIN) and two sample and hold circuits for storing the signal level and the reset level. Sampling both the reset and signal levels permits correlated double sampling (CDS) which suppresses reset noise from the floating diffusion node of the pixel, and 1/f noise and threshold variations from the source-follower transistor within the pixel.³²⁻³⁴ Each sample and hold circuit consists of a sample and hold switch (MSHS or MSHR) and capacitor (CS or CR) and a column source-follower (MP1 or MP2) and column selection transistor (MY1 or MY2) to buffer the capacitor voltages and to drive the high capacitance horizontal bus at higher readout speeds. The load transistors of the column source-followers (MP1 and MP2) are common to the entire array of pixels. P-channel source-followers are used in the column circuit to compensate for the level shifting of the signal due to n-channel source followers within the pixels. The summary of the CMOS APS is given in table 1,

Table 1

Transistor and Capacitor Sizes

Element	Function	Size
MR	ltd-pixel reset transistor	3/2
MIN	In-pixel Source-follower input	6/2
MX	Row-selection switch	6/2
MLN	First source-follower load	3/4
MSHR,MSHS	Sample and hold switches	3/2
MP1,MP2	Column source-follower inputs	120/2
MY1,MY2	Column-selection switches	120/2
MLP1,MLP2	Second source-follower loads	30/2
MCB	Crowbar switch	3/2
MS1,MS2	Crowbar selection switches	3/2
CS,CR	Sample and hold capacitors	1pF
CS, CR	Modified sample and hold capacitors	2.3 pF

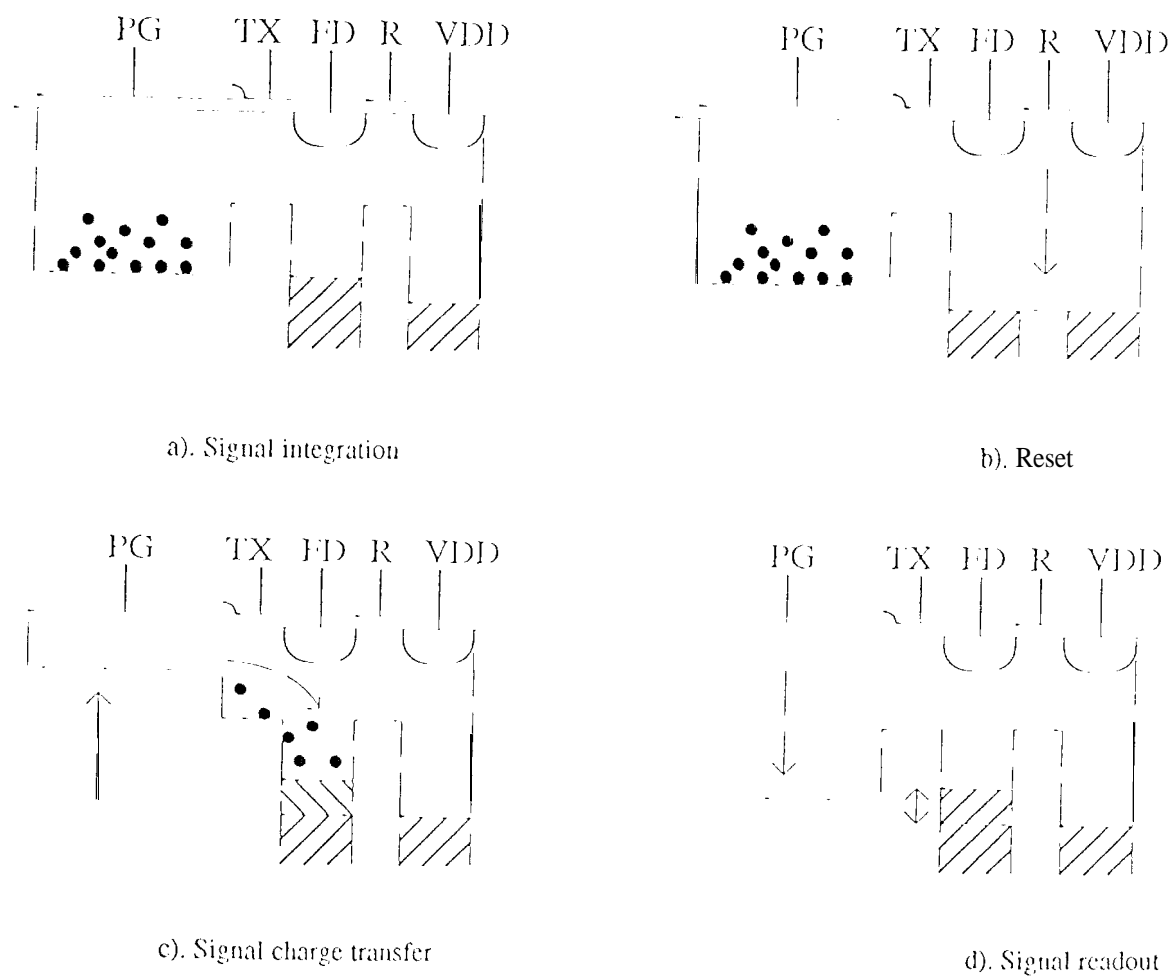


Figure 4. Operation of CMOS APS

The operation of this image sensor is illustrated in Figs. 4(a)-(d). The rail voltages V_{DD} and V_{SS} are set at 5V and 0 V respectively, and the transfer gate TX is biased at 2.5V. The load transistors of the in-pixel source-follower and the column source-followers (M1.N, M1.P1 and M1.P2 in Fig. 3) are d.c. biased at 1.5V and 2.5V respectively. During the signal integration period (Fig. 4(a)), photogenerated electrons are collected under the surface-channel photogate PG biased at 5V. The reset transistor MR is biased at 2.5V to act as a lateral anti-blooming drain, allowing excess signal charge to flow to the reset drain. The row-selection transistor MX is biased off at 0 V. Following signal integration, an entire row of pixels are read out simultaneously. First, the pixels in the row to be read out are addressed by enabling row selection switch MX. Then the floating diffusion output node of the pixel (FD) is reset by briefly pulsing the reset gate of MR to 5V. This resets FD to approximately 3.5V (Fig. 4(b)). The output of the first source-follower is sampled onto capacitor CR at the bottom of the column by enabling sample and hold switch MS1R. Then, PG is pulsed low to 0 V, transferring the signal charge to FD (Fig. 4(c)). The new output voltage is sampled onto capacitor CS by enabling sample and hold switch MS1S (Fig. 4(d)). The stored reset and signal levels are sequentially scanned out through the second set of source-followers by enabling column address switches MY1 and MY2. This timing sequence is shown in Fig. 5.

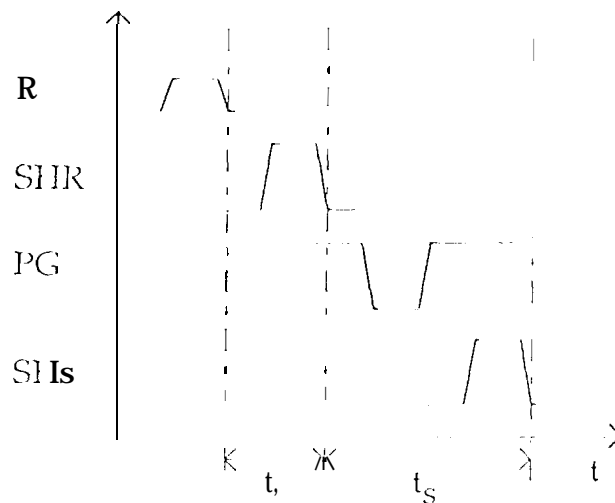


Figure 5. Timing for CMOS AFSS Readout

4. Challenges

The objective of this research is to develop a forward looking focal plane array sensor closely aligned on a monolithic active pixel frame in two different selected paired hyper spectral bands (one in visible for physical observation and another for functional scanning in 2.0 - 2.5 μm transmission spectral window of air) for clutter reduction and enhancement of the desired features for Navy application in remedial action control, surveillance, and precision strike.

The success of this proposal depends heavily on the sensing and readout structure. The bus, optimization of the major parts, such as the selection of InGaAs material, fabrication capability of the reliable JFET structure for the design of active pixel sensors. Effective design of the readout circuit, is also vital factor to successfully integrate the system to detect the multispectral sensor arrays.

Since it is not intended to grow the material at JPL in this proposal, MBE grown InGaAs on InP substrates will be obtained from outside of the Laboratory at best available bases. Several different superlattice (refer Figure 1) wafers with $\text{In}_{1-x}\text{Ga}_x\text{As}$, including $\text{In}_{0.53}\text{Ga}_{0.47}\text{As}$ and $\text{In}_{0.52}\text{Ga}_{0.48}\text{As}$, will be also obtained and characterized in an effort to select proper spectral range of 1.3 - 2.5 μm by Fourier Transformation Infrared Spectrometer at the JPL's Infrared Sensor Laboratory. Simple active pixel sensor circuits (Figure 3) consisted of JFETs will be designed at the JPL's VLSI design Laboratory and be fabricated at the Microelectronic Devices Laboratory at JPL. Measurement of temperature dependence of fabricated devices in optical and electrical device response will be performed using infrared imager testbed. Pulse Instruments and by

Multipurpose Microelectronic Advanced Laser Scanner at JPL. The conventional lock-in amplifying system together with active readout electronics will be applied without miniaturization for the first Phase one-year feasibility research.

Infrared and visible focal plane arrays are the critical components in existing and future mobile weapon systems for night and day vision in Navy activities. Dual IR scanning systems were only applied for enhancing the desired features in surveillance. However, the physical (visible) and functional (IR) images of the same object obtained by the same focal plane arrays are vital to an operator to take immediate action without extra processing of the data from two different sensor arrays. This can be achieved by the active pixel dual (VIS/IR) bands staring focal plane arrays even near room temperature. This could be a revolutionary technology for a wide range of correctional action, improving spatial as well as temporal profiles for field surveillance and missile warning.

If this effort is successful, the following two years will be concentrated to integrate a prototype of a miniaturized, and mobile system for the technology transfer.

5. ACKNOWLEDGMENTS

The authors appreciate the assistance of Drs. T. N. Krabach and B. T'sill of JPL and Dr. G. Olsen of Sensors Unlimited in discussions. This work was supported by the grants of the ONR N00014-97-1-0041 and JPL 2(M-1B)02. The research described in this paper was carried out by the Jet Propulsion Laboratory, California Institute of Technology, under a contract with the National Aeronautics and Space Administration. Reference herein to any specific commercial product, process, or service by trade name, trademark, manufacturer, or otherwise, does not constitute or imply endorsement by the United States Government or the Jet Propulsion Laboratory, California Institute of Technology.

6. REFERENCES

1. J. K. Notthoff and R. Zuleeg, "High Speed Low-Power GaAs JFET Integrated Circuits", *IEEE Tech. Digest*, p.624, 1975
2. C. L. Lin, J. M. Fernandez, and H. H. Wieder, "An anisotype GaAs/InGa_{1-x}As Heterojunction Field-Effect Transistor for digital Logic Applications", *IEEE, EDL*, vol 11, p.1810, 1990
3. A. I. Akinwande et al., "Complementary II-V Heterostructure FET's for Low Power Integrated Circuits", *IEEE Tech Digest*, p.893, 1990
4. K. Lee and S. H. Shur, "π-heterostructure Field Effect Transistors for VLSI Applications", *IEEE Trans., ED*, vol 37, p.1810, 1990
5. S. B. T. Jeon, J. H. Han, K. Lee, and Y. S. Kwon, "Self-aligned Shallow Junction MJFET for Higher Turn-on and Breakdown Voltages", *IEEE, EDL*, vol 13, p.630, 1992
6. T. Takada, N. Kato, and M. HDA, "An 1.1ghz GaAs Frequency Divider Using Source-coupled FET Logic", *IEEE ED Lett.*, vol. 7, p.47, 1986
7. J. F. Jensen, L. G. Salmon, D. S. Deakin, and M. J. Delanoy, "Ultra High Speed GaAs Static Frequency Dividers", *IEEE Tech Digest*, p.476, 1986
8. E. R. Fossum, "Active Pixel Sensors: Are CCD's Dinosaurs?", *Proceed. of SPIE*, Vol. 1900, Charge-Coupled Devices and Solid-State Optical Sensors III (1993)
9. M. L. Eastwood, C. M. Sarture, T. G. Chrien, R. O. Green, W. M. Porter, "Current instrument status of the airborne visible/infrared imaging spectrometer (AVMIS)", *Proc. SPIE*, Vol. 1540, pp. 161-175 (1991).
10. J. B. Wellman, J. Duval, D. Juergens, J. Voss, "Visible and infrared mapping spectrometer (VIMS): a facility instrument for planetary missions", *SPIE*, Vol 834, p. 213 (1987).
11. G. H. Olsen, "InGaAs fills the near-IR detector-array vacuum", *Laser Focus World*, Vol 27(3), pA21 (1991).
12. V. S. Ban, K. Woodruff, M. Lange, G. Olsen, and K. A. Jones, "Comparison of InGaAs/InP p-i-n detectors grown by hydride and organometallic vapor phase epitaxy", *IEEE Transactions on Electron Devices*, Vol 37(3), p814 (1990).
13. K. R. Linga, G. H. Olsen, V. S. Ban, A. M. Joshi, and W. F. Kosonocky, "Dark current analysis and characterization on InGa_{1-x}As/InAs VPI-y graded photodiodes with x>0.53 for response to longer wavelengths (>1.7 μm)", *IEEE Journal of Lightwave Technology*, Vol. 10(8), p 1050 (1992).

14. K. I. Kavanagh, J. C. P. Chang, J. Chen, J. M. Fernandez, and H. H. Wieder, "Lattice tilt and dislocations in compositionally step-graded buffer layers for mismatched InGaAs/GaAs heterointerfaces," *J Vac. Sci. Tech. B* Vol 10(4), p1820 (1992).
15. J. Chen, J. M. Fernandez, J. C. P. Chang, K. I. Kavanagh, and H. H. Wieder, "Modulation-doped In_{0.3}Ga_{0.7}As/In_{0.29}Al_{0.71}As heterostructures grown on GaAs by step grading," *Semicond. Sci. Tech.* Vol 7, p601 (1992).
16. N. C. Tien, J. Chen, J. M. Fernandez, and H. H. Wieder, "Unstrained, Modulation-Doped, In_{0.3}Ga_{0.7}As/In_{0.29}Al_{0.71}As field-effect transistor grown on GaAs Substrate," *IEEE Electron Device Letters*, Vol 13 (12), p621 (1992).
17. D. L. Rogers, J. M. Woodall, G. D. Pettit, and D. McInturff, "High-speed 1.3 μ m GaInAs detectors fabricated on GaAs substrates," *IEEE Electron Device Letters*, Vol 9(10), p515 (1993).
18. T. J. Shealy, M. Matloubian, T. Y. Liu, M. A. Thompson, M. M. Hashemi, S. P. Denbaars, and U. K. Mishra, "High-Performance Submicrometer Gate-length GaInAs/InP Composite Channel HEMT's with Regrown Ohmic Contacts," *IEEE Electron Lett.*, vol. 17, p540 (1996).
19. J. J. Kozlowski, K. Vural, W. H. Tennant, R. Kezer, and W. J. Kleinhaus, "Low Noise 2.5 μ m PACF-1 HgCdTe IOx132 FPA with 25 μ m Pitch and On-Chip Signal Processing Including CDS and '1'1," *Proceedings of IRIS Specialty Group on Infrared Detectors Vol. II, NIST, Boulder, CO*, p. 155.
20. T. N. Krabach, C. Staller, S. Dejewski, T. Cunningham, M. Herring, and E. R. Fossum, "InGaAs Detector for Miniature Infrared Instruments," *Proceed. of the SPIE*, Vol. 1874, Infrared and Millimeter Wave Engineering, p. 33 (1992).
21. E. R. Fossum, "Architectures for focal-plane image processing," *Optical Engineering*, vol. 28(8), pp. 865-871, August 1989.
22. S. E. Kemeny, E. S. Eid, S. Mendis and E. R. Fossum, "Update on focal-plane image processing research," *Charge-Coupled Devices and Solid-State Optical Sensors II, Proc. SPIE*, vol. 1447, pp. 243-250, February 1991.
23. A. M. Chiang and B. E. Burke, "A High Speed Digitally Programmable CCD Transversal Filter," *IEEE J. Solid-State Circuits*, vol. 18, pp. 745-13, September 1983.
24. D. Renshaw, P. Denyer, G. Wang and M. Liu, "ASIC vision," *Proc. IEEE Custom Integrated Circuits Conference*, pp. 7.3.1-7.3.4, 1990.
25. F. Andoh et al., "A 250,000-Pixel Image Sensor with FET Amplification at Each Pixel for High-Speed Television Cameras," *ISSCC Digest of Technical Papers*, pp. 212-213, February 1990.
26. M. Ogata, T. Nakamura, K. Matsumoto, R. Ohta and R. Hyuga, "A small pixel CMOS image sensor," *IEEE Trans. Electron Devices*, vol. 37(4), pp. 964-971, April 1990.
27. J. Hynecek, "BCMD - An improved photosite structure for high density image sensors" *IEEE Trans. Electron Devices*, vol. 38(5), pp. 1011-, May 1991.
28. N. Tanaka, T. Ohmi and Y. Nakamura, "A novel bipolar imaging device with self-noise reduction capability," *IEEE Trans. Electron Devices*, vol. 36(1), pp. 31-37, January 1989.
29. J. Nisizawa, T. Tamamushi and T. Ohmi, "Static induction transistor image sensor," *IEEE Trans. Electron Devices*, vol. 26(12), pp. 1970-1977, December 1979.
30. R. Nixon, S. Kemeny, C. Staller and E. Fossum, "128x128 CMOS photodiode-type active pixel sensor with on-chip timing, control and signal chain electronics," *Charge-Coupled Devices and Solid-State Optical Sensors V, Proc. SPIE*, vol. 2415, paper no. 34, February 1995.
31. S. K. Mendis, S. E. Kemeny, R. C. Gee, B. Pain, C. O. Staller, Q. Kim, and E. R. Fossum, "CMOS Active Pixel Image Sensors for Highly Integrated Imaging Systems", to be published in *IEEE Trans.*
32. M. White, D. Lampe, F. Blaha and I. Mack, "Characterization of surface channel CCD image arrays at low light levels," *IEEE J. Solid-State Circuits*, vol. 9, pp. 1-13, September 1974.
33. J. Hynecek, "A New Device Architecture Suitable for High-Resolution and High Performance Image Sensors," *IEEE Trans. Electron Devices*, vol. 35, no. 5, May 1988.
34. N. Tanaka et al. "A 310k Pixel Bipolar Imager (BASIS)," *ISSCC Digest of Technical Papers*, pp. 96-97, February 1989.